



Contents lists available at ScienceDirect

Spectrochimica Acta Part A: Molecular and Biomolecular Spectroscopy

journal homepage: www.elsevier.com/locate/saa

The investigation of unique water-soluble heptamethine cyanine dye for use as NIR photosensitizer in photodynamic therapy of cancer cells

Xin Yang, Jin Bai, Ying Qian *

School of Chemistry and Chemical Engineering, Southeast University, Nanjing, 211189, China

ARTICLE INFO

Article history:

Received 6 July 2019

Received in revised form 17 October 2019

Accepted 24 October 2019

Available online xxx

Keywords:

Water-soluble dye

NIR photosensitizer

Photodynamic therapy

Heptamethine cyanine

ABSTRACT

In this paper, a unique water-soluble heptamethine cyanine dye as NIR photosensitizer was synthesized to explore its properties associated with potential applications in photodynamic therapy (PDT). In the strategy of designing this photosensitizer, a sulfonic acid was used as a water soluble functional group and linked to the fluorophore through alkyl chains. 4-amino-2,2,6,6-tetramethylpiperidine-N-oxyl(Tempo) moiety was used as the a nitroxide spin label in obtaining biochemical reaction information in vivo due to it could greatly increase the inter-system crossing (ISC) process for triplet-state photosensitizers and low toxicity. As expected, the photosensitizers performed well in vitro photodynamic therapy. There were a remarkable absorbance band located at 692 nm and emission peaks falls at 762 nm, the quantum yield (Φ_T) was calculated to be 12.12% in pure aqueous solution using ICG as standards. The photosensitizer also has high singlet oxygen quantum yield (Φ_Δ) for 16.96% with NIR LED irradiation. This photosensitizer can rapidly produce singlet oxygen and exhibit high phototoxicity under NIR light irradiation. It has excellent cellular uptake ability and better cell compatibility. It was also successfully applied in Near-infrared fluorescence imaging and AO/EB staining. In a whole, the organic dye based on Heptamethine cyanine used as photosensitizer has great potential in vivo cancer treatment.

© 2019 Elsevier B.V. All rights reserved.

1. Introduction

Photodynamic therapy (PDT) is a new method of treating tumor diseases with photosensitizers and laser activation [1–4]. During processing, the photosensitizer transfers energy to the surrounding oxygen and produces highly active singlet oxygen. Subsequently, singlet oxygen can react with nearby bio-macromolecules through oxidation reaction, producing cytotoxicity and killing tumor cells [5–8]. Photosensitizers are essential in photodynamic therapy [9,10]. The excellent photosensitizers should possess low dark toxicity and highly reactive under appropriate irradiation. In recent years, great efforts of the researchers have been exert to develop photosensitizers with large molar extinction coefficient, high inter-system crossing (ISC) efficiency, and good photostability [11]. However, most of the photosensitizer exhibits high dark toxicity, owing to their absorbance and emission wavelength was located in visible region rather than the NIR region [12]. There were many advantages of the photosensitizers irradiated by near-infrared (NIR) light [13–15], such as, working in the NIR optical window can provide a deeper irradiation depth and highly reactive [16–21]. There were still many fluorophore has great potential to explore as photosensitizers [22–24]. As a result, it is still a challenge for the researchers to explore

photosensitizers with low dark toxicity but prominent phototoxicity under irradiation for PDT.

Heptamethine cyanine, one of the most common organic dyes, has become a more promising tool for cancer imaging and targeted therapy owing to their stability and versatility with absorption in the near-infrared region (NIR) of the electromagnetic spectrum upon modification [25–27]. Those dyes have many advantages when used as fluorophore. However, when those dyes were used as photosensitizers for PDT, they have low phototoxicity owing to singlet oxygen (1O_2) quantum yields was very low, such as the singlet oxygen (1O_2) quantum yields of IR-783 and ICG are 0.007 and 0.008, respectively [28]. Therefore, the organic fluorophores were generally modified by chemical synthesis, usually introducing heavy atoms to increase singlet oxygen generation efficiency [29–31]. Nthabeleng [32] et al has design and synthesis a photosensitizer based on BODIPY for PDT. The structure was introduced Br atom to increase the singlet oxygen quantum yield. However, while increasing the yield of singlet oxygen, it also produces higher dark toxicity [33]. Jiao [34] et al has synthesis a photosensitizer based on heptamethine aminocyanine dye for PDT, the photosensitizer shows high singlet oxygen quantum yield for 0.2 after 40 s irradiation. As a result, it is essential for the researcher to explore a new NIR heavy-atom-free photosensitizers with satisfactory inter system crossing, high singlet oxygen (1O_2) yields and low dark toxicity for fast killing the cancer cells.

* Corresponding author.

E-mail address: yingqian@seu.edu.cn (Y. Qian).

Keep those problems in mind, a unique organic NIR dye based on heptamethine cyanine with heavy-atom-free and water soluble functional group was designed and synthesized for photodynamic therapy. The photosensitizer was estimated has many advantages when used for PDT, such as it can work in pure water solution, it has better biocompatible and high singlet oxygen ($^1\text{O}_2$) quantum yields, low dark toxicity and so on. In the designing strategy of photosensitizer, 2,2,6,6-Tetramethylpiperidinyloxy moiety was incorporated into a fluorophore due to its response to the singlet oxygen ($^1\text{O}_2$) and it can increase the inter-system crossing (ISC) process for triplet-state photosensitizers and low toxicity. It greatly improved the PDT efficiency by NIR light photo damage induced cell death [35]. Heptamethine cyanine was elected as fluorophore owing their stability and versatility with absorption in the near-infrared (NIR) region, high extinction coefficient, low biological toxicity and good biocompatibility. We anticipated that this photosensitizer has great capacity to provide attractive results for the treatment of tumor cells (Scheme 1).

2. Experimental section

2.1. Materials and methods

2.1.1. MTT assay for *in vitro* dark cytotoxicity studies

The dark toxicity of the two dyes (CyO^- and CyOH) were evaluated by MTT assay before *in vitro* photodynamic therapy studies using HepG-2 cells. The HepG-2 cells were cultured using 90% DMEM medium and 10% fetal bovine serum under 5% CO_2 at 37 °C until the density of cells reached 2×10^6 cells per mL. Then the HepG-2 cells were seeded in 96-well plates and incubated at 37 °C, 5% CO_2 for 24 h to allow the cells to adhere. Then added different concentration of dyes to each well and continue to incubate for another 24 h under the same condition. Then add new medium continue to culture the cells for 12 h before testing. Eventually, the cells were injected with 5 mg mL^{-1} MTT for 4 h at the condition mentioned above. The supernatant was then discarded, 100 mL DMSO was added to each well and oscillation was conducted for 5 min. The absorbance of each well of the 96-well plate was then assessed at 490 nm on a Benchmark Plus plate reader.

2.1.2. MTT assay for *in vitro* photodynamic therapy studies

The *in vitro* photodynamic therapy studies was carried out using MTT assay as described in the previously section. The different was after added different concentration of dyes to each well and continue to incubate for another 24 h, the fresh medium was added and irradiated by NIR LED lamp for 30 min and cultured for 12 h. MTT array was tested on HepG-2 cells. The dark cytotoxicity was monitored without irradiation at the same time as control.

Cell viability was calculated according to the equation [36]: cell viability (%) = average value of sample OD490/average value of blank OD490 \times 100%, where, OD490 is the absorbance measured at 490 nm.

2.1.3. Acridine orange (AO)/ethidium bromide (EB) staining assay

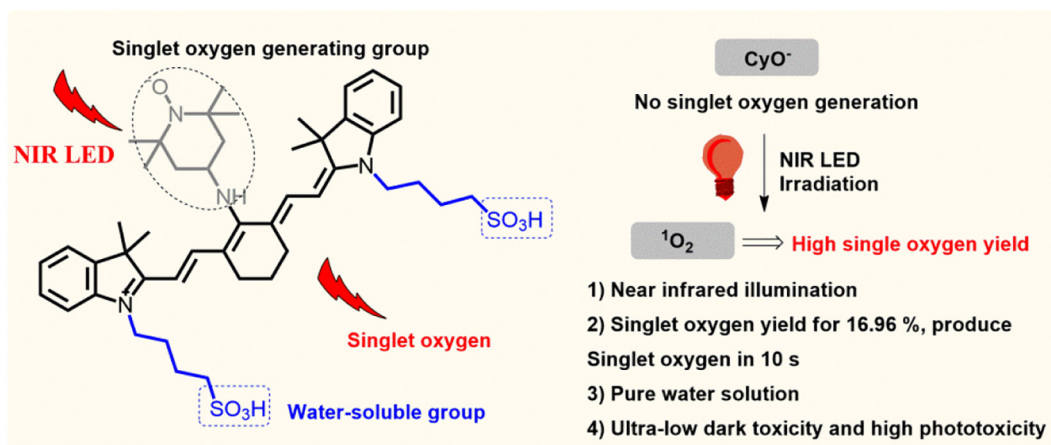
HepG-2 cells were seeded on a glass bottom confocal dish for 12 h under the condition of 37 °C and 5% CO_2 . The dye of CyO^- (20 μM) was incubated with HepG-2 cells for 12 h under the same condition. During the PDT process, the ice pack was placed under the glass bottom confocal dish to eliminate the effects of elevated temperatures. Then group A with no CyO^- was irradiated for 20 min, group B was co-incubated with CyO^- for 12 h and with no irradiation. Group C with CyO^- was irradiated for 20 min and immediately stained with AO/EB. Group D with CyO^- was irradiated for 20 min and continue to train for 1 h. After the above treatment, the cells were washed three times with PBS buffer. 500 μl of staining buffer was added to the glass bottom dish, immediately after, 5 μl AO staining solution and 5 μl EB staining solution were added to cell suspension mentioned above and incubate for 15 min at room temperature, protected from light.

2.1.4. Confocal fluorescence microscopy

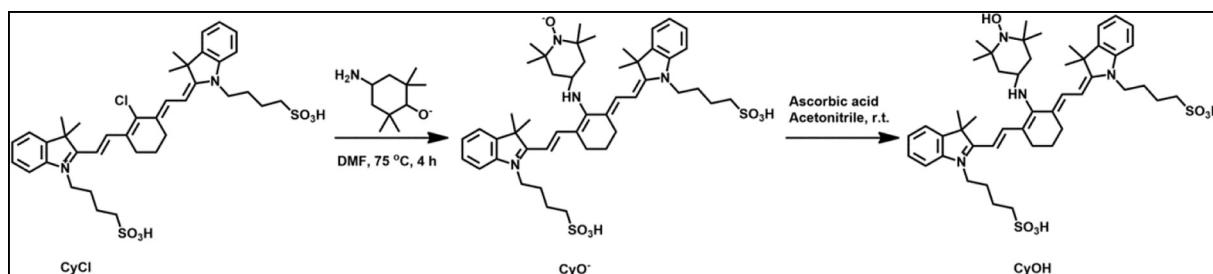
Fluorescence imaging was performed on a confocal laser scanning microscope (FLUOVIEW FV3000. OLYMPUS). The MCF-7 cells were seeded on a glass bottom confocal dish for 12 h and co-incubated with CyO^- for another 12 h under the condition of 37 °C and 5% CO_2 . The cells were washed three times with PBS and then stained with DAPI for 10 min. Subsequently, the cells were washed three times with PBS to remove excess DAPI staining solution. Finally, confocal imaging was conducted on confocal laser scanning microscope.

2.1.5. Singlet oxygen quantum yields

The singlet oxygen quantum yield was measured using methylene blue (MB) as the standard in ethanol solution and examined using 1,3-diphenylisobenzofuran (DPBF) as a $^1\text{O}_2$ probe. At the beginning, DPBF was dissolved in ethanol to adjust the concentration to make sure the absorbance at 411 nm was about 1. The four dyes were dissolved in ethanol, and the absorbance was adjusted so that the absorbance at the maximum absorption peak was between 0.2 and 0.3, and the light was irradiated with monochromatic NIR light, and the absorbance of DPBF at 411 nm was recorded every 1 s. According to the same method, the singlet oxygen production rate of MB was measured, and the change of the absorbance at 411 nm was plotted on the ordinate and the irradiation time was plotted on the abscissa to obtain the slope. Finally, the calculation of the singlet oxygen quantum efficiency is performed according to the following



Scheme 1. The design of new NIR photosensitizer.



Scheme 2. The route of synthesis new photosensitizer.

formula: $\frac{\Phi_{\Delta} = \Phi_{\Delta}(MB) \times K_{Dye}}{K_{MB} \times F_{MB}}$, where k is the slope between absorbance and the irradiation time, F is the correction of dye and reference absorbance, where $F = 1 - 10^{-OD}$

2.2. Synthesis

The synthesis of unique NIR photosensitizer was depicted in [Scheme 2](#). It takes five steps to complete its composition, as follows.

2.2.1. 4-((E)-2-((E)-2-(3,3-dimethyl-1-(4-sulfobutyl)-3H-indol-1-ium-2-yl)vinyl)-6-((E)-2-(3,3-dimethyl-1-(4-sulfobutyl)indolin-2-ylidene)ethylidene)cyclohex-1-en-1-yl)amino)-2,2,6,6-tetramethylpiperidin-1-olate (CyO⁻)

2-((E)-2-((E)-2-chloro-3-((E)-2-(3,3-dimethyl-1-(4-sulfobutyl)indolin-2-ylidene)ethylidene)cyclohex-1-en-1-yl)vinyl)-3,3-dimethyl-1-(4-sulfobutyl)-3H-indol-1-ium (0.1 g, 0.14 mmol) and 4-amino-2,2,6,6-tetramethylpiperidin-1-olate (0.071 g, 0.42 mmol) were dissolved in anhydrous DMF (5 mL) and stirred at 75 °C for 4 h under N₂ atmosphere. The crude product was obtained through steaming off DMF. Eventually, the crude product was purified by thin layer chromatograph to afford pure solid. ¹H NMR (300 MHz, DMSO-*d*₆): δ 7.95 (s, 1 H), 7.78 (s, 1 H), 7.48 (d, $J = 12.9$ Hz, 2 H), 7.32 (m, 8 H), 5.96 (s, 1 H), 5.75 (s, 1 H), 4.02 (d, $J = 25.8$ Hz, 6 H), 3.62 (m, 8 H), 2.89 (s, 3 H), 2.73 (s, 3 H), 1.93 (d, $J = 13.8$ Hz, 4 H), 1.72 (m, 12 H), 1.24 (s, 4 H), 1.12 (m, 12 H) HRMS calcd for C₄₇H₆₆N₄O₇S₂ 862.43729, found: 862.43639.

2.2.2. 2-((E)-2-((E)-3-((E)-2-(3,3-dimethyl-1-(4-sulfobutyl)indolin-2-ylidene)ethylidene)-2-((1-hydroxy-2,2,6,6-tetramethylpiperidin-4-yl)amino)cyclohex-1-en-1-yl)vinyl)-3,3-dimethyl-1-(4-sulfobutyl)-3H-indol-1-ium (CyOH)

Dye2 (50 mg, 0.058 mmol) and ascorbic acid (51.05 mg, 0.29 mmol) were added to the 50 mL round-bottomed flask using acetonitrile as

the solvent. Then, the mixture was stirred at room for 30 min under N₂ atmosphere. The solvent was removed by rotary evaporation and purified by Column chromatography to afford the purple solid 50.0 g. Yield: 97.8% (¹H NMR (300 MHz, DMSO-*d*₆): δ 7.92 (s, 1 H), 7.76 (d, $J = 13.5$ Hz, 2 H), 7.46 (d, $J = 7.5$ Hz, 2 H), 7.29 (m, 4 H), 7.10 (t, $J_1 = 7.2$ Hz, $J_2 = 7.2$ Hz, 2 H), 6.9 (s, 1 H), 5.94 (d, $J = 12.6$ Hz, 2 H), 5.71 (d, $J = 28.2$ Hz, 1 H), 3.99 (d, $J = 24.9$ Hz, 4 H), 3.71 (t, $J_1 = 6.6$ Hz, $J_2 = 6.9$ Hz, 10 H), 2.85 (s, 1 H), 2.69 (s, 1 H), 1.72 (s, 8 H), 1.59 (s, 9 H), 1.34 (m, 12 H), 1.04 (t, $J_1 = 6.9$ Hz, $J_2 = 6.9$ Hz, 7 H) HRMS calcd for C₄₇H₆₇N₄O₇S₂⁺ 863.44457, found: 863.44440.

3. Results and discussion

3.1. Design strategy of unique water soluble NIR photosensitizers with TemOH functional group and long emission wavelength for PDT

The synthetic route of photosensitizers was reported previously [37]. The unique NIR photosensitizer was prepared via five steps as shown in [Scheme 2](#). Heptamethine cyanine was selected as the basic fluorescent core due to its absorbance and emission wavelength located in near red region and it has low toxicity. Water-soluble functional group was linked to fluorescent core through alkyl chain. 4-amino-2,2,6,6-tetramethylpiperidin-1-olate moiety was used as the a nitroxide spin label in obtaining biochemical reaction information in vivo due to it could greatly increase the intersystem crossing (ISC) process for triplet-state photosensitizers and low toxicity. It was introduced to Heptamethine cyanine moiety through nucleophilic substitution reaction. Eventually, new NIR photosensitizer was constructed. We anticipated that the photosensitizer has excellent properties such as Ultra low dark toxicity and higher singlet oxygen production efficiency, better biocompatibility.

All intermediates and target products were passed nuclear magnetic resonance spectroscopy and high resolution mass spectrometry (Supporting information [Fig. S1-Fig. S5](#)) ([Scheme 2](#)).

3.2. Production of singlet oxygen of near-infrared heptamethine cyanine dye

The basic fluorescence spectrum and UV-visible spectrum properties was investigated in pure aqueous solution. As shown in [Fig. 1](#), there were three remark absorption peak located in 776 nm, 692 nm, 686 nm for CyCl, CyO⁻, CyOH, respectively, which of them were all reached to NIR regions, it's of great value to cell imaging. The molar extinction coefficient was worked for 2.56×10^5 M⁻¹ cm⁻¹, 1.42×10^5 M⁻¹ cm⁻¹, 0.43×10^5 M⁻¹ cm⁻¹, for CyCl, CyO⁻, CyOH, respectively. The emission wavelength of three

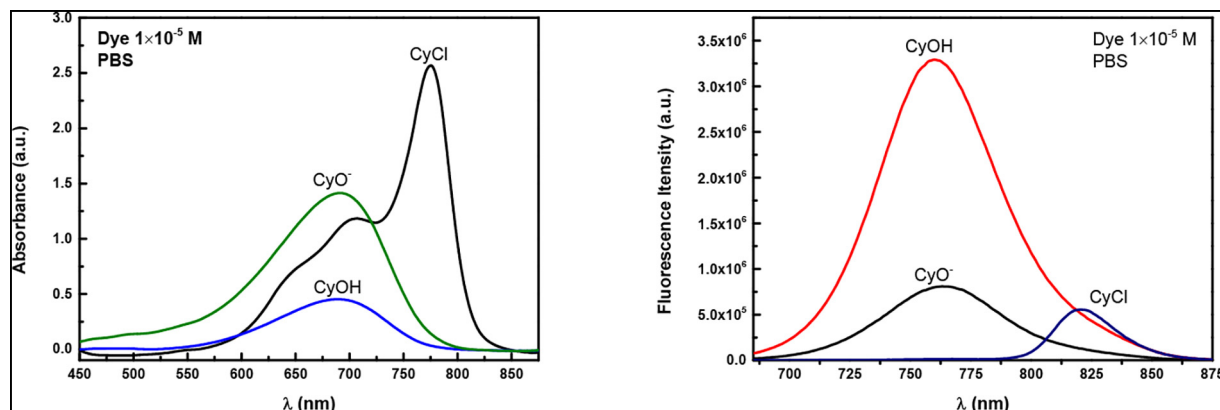


Fig. 1. The fluorescence response and absorbance response of CyO⁻, CyOH, CyCl (10 μM) in PBS (pH= 7.4) and ethanol.

Table 1
The detailed photophysical properties of new photosensitizers

Dye	λ_{abs} (nm)	E_{max} (10 ⁵ M ⁻¹ cm ⁻¹)	λ_{em} (nm)	Φ_f	Φ_{Δ}
CyO ⁻	692	1.42	762	12.12%	16.96%
CyOH	686	0.43	759	1.98%	1.98%
CyCl	776	2.56	821		1.89%

MB as a reference for singlet oxygen quantum yield measured. ICG was used as a standard for quantum yield measure. Where Φ_{Δ} represent Singlet Oxygen quantum yield, Φ_f represent quantum yield.

dyes were also located in 821 nm, 762 nm, 759 nm for CyCl, CyO⁻, CyOH, respectively. The results show that the probe has a good absorption capacity for near-infrared light and has a broad application in photodynamic therapy (see).

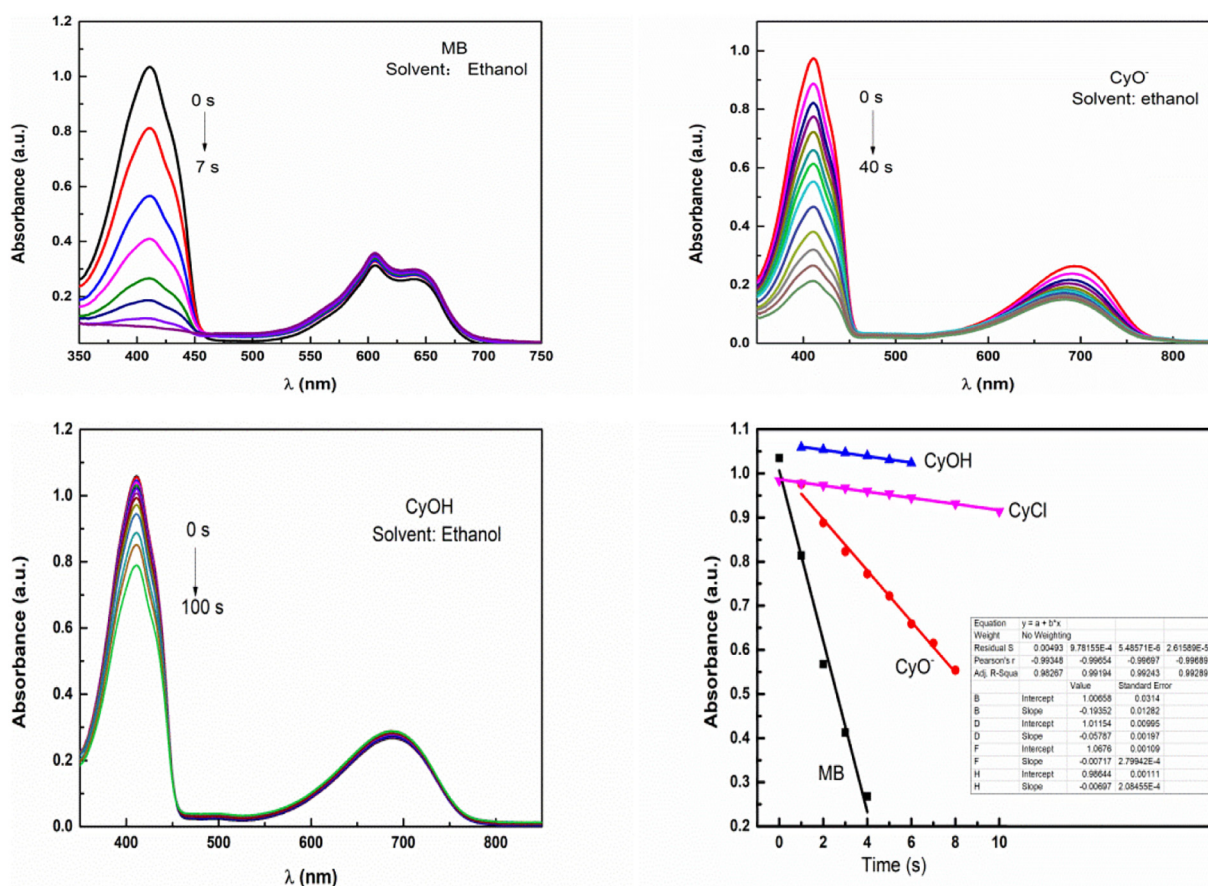


Fig. 2. Comparison of DPBF bleaching rate at 411 nm. Near infrared LED array irradiation for different time. CyO⁻ and CyOH were dissolved in ethanol and mixed with DPBF to a suitable concentration.

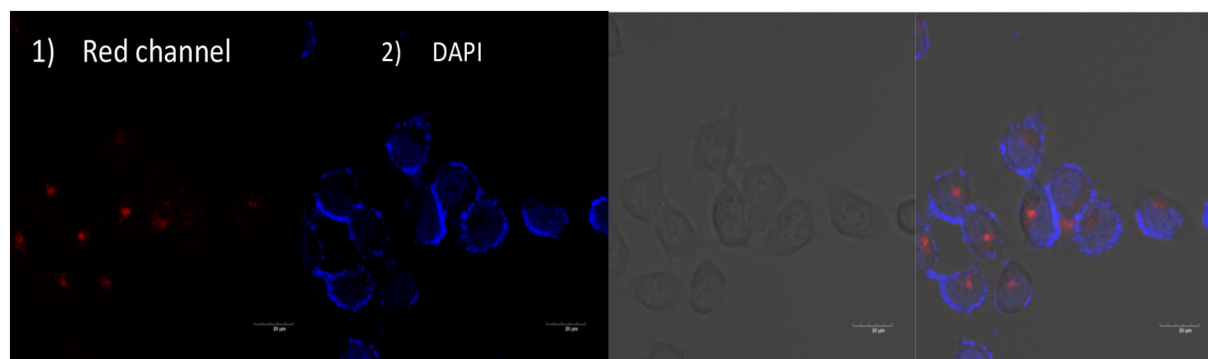


Fig. 3. Confocal images of MCF-7 cells of DAPI- stained cells with pre-incubated with CyO⁻ (10 μ M). Scale bar = 20 μ m.

NIR dyes are highly sought owing to their excellent properties in chemical biology. In contrast with visible light, NIR light has more potential applied in biological imaging and PDT process due to their deep tissue penetration, minimum photodamage to biological samples, and minimum interference from background auto-fluorescence by biomolecules in the living systems. However, NIR dyes generally sacrifice quantum yields by adopting the loose π -conjugated structures. So the quantum yield of CyO⁻ was evaluated using ICG as reference. The quantum yield was calculated for 12.12% in pure aqueous solution using the equation [38]: $\phi_x = \phi_s \left(\frac{K_x}{K_s} \right) \left(\frac{n_x}{n_s} \right)^2$, where $K_x = \frac{F_x}{A_x}$, $K_s = \frac{F_s}{A_s}$, F is Fluorescence area, A is absorbance, x and s represent standard and test solution. It's higher than the reported NIR dye. The results demonstrated that the CyO⁻ has great advantage in bio-imaging (Table 1).

3.3. Comparison of singlet oxygen yields of three probe molecules

The evidence confirmed that the production of reactive oxygen species (ROS) is closely related to the excited triplet state of photosensitizers. It's estimated that the

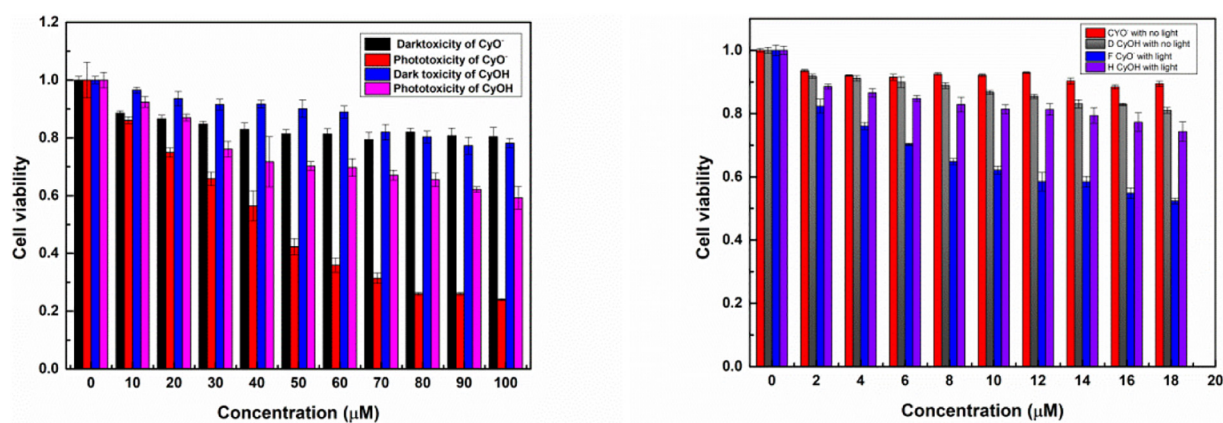


Fig. 4. Dark toxicity and phototoxicity evaluation of CyO⁻ and CyOH on HepG-2 cells for 30 min irradiation (NIR light). MTT array was measured after incubating for 12 h with different concentration of two dyes. Data are presented as the mean value \pm SD ($n = 6$).

presence of heptamethine cyanine dye's longevity triplet excited state interacts with molecular oxygen ($^3\text{O}_2$) to form singlet oxygen ($^1\text{O}_2$), which may be useful for PDT applications. Singlet oxygen generation was examined using 1,3-diphenylisobenzofuran (DPBF) as a $^1\text{O}_2$ probe. As shown in Fig. 3, in presence of CyO⁻, the absorbance of DPBF shows a significant drop at 411 nm under irradiation of NIR light (670 nm), confirming their ability to generate $^1\text{O}_2$. In contrast, CyOH and CyCl showed a small reduction in absorption at 411 nm under the same conditions even could negligible. Those results strongly confirmed that introducing 4-amino-TEMPO into a Heptamethine cyanine dye can remarkably enhance the ability of $^1\text{O}_2$ generation, mainly originated from the formation of the triplet state (T1) from Heptamethine cyanine dye. In order to quantitatively measure the singlet oxygen production efficiency of the three dyes, the singlet oxygen efficiency measurement was carried out. Methylene blue was used as a reference in ethanol and the singlet oxygen quantum yields was calculated for 16.96% and 1.98%, 1.89% of CyO⁻, CyOH, CyCl respectively according to the equation: $\Phi_{\delta} = \Phi_{\delta}(\text{MB}) \times \frac{K(\text{dye})}{K(\text{MB})} \times \frac{F(\text{MB})}{F(\text{dye})}$. The singlet oxygen

production efficiency of this dye is significantly higher than the previously mentioned IR-783 and ICG are 0.007 and 0.008. It has great potential applied in photodynamic therapy (Fig. 2).

The cellular uptake property of CyO⁻ was measured in MCF-7 cells using confocal imaging. As shown in Fig. 3, the CyO⁻ could get into MCF-7 cells and showed a strong red fluorescence under NIR light excitation. The clear red channel illustrate that the CyO⁻ can easily uptake by MCF-7 cells and it has great ability to penetrate cell with good cell compatibility (Fig. 3).

3.4. Cell study for dark toxicity and photo toxicity

To evaluated the photodynamic therapy effect of CyOH and CyO⁻, dark toxicity and phototoxicity was carried out by MTT (3-(4,5-dimethylthiazol-2-yl)-2,5-diphenyl-tetrazole) assay in the dark and the light irradiation, respectively. As shown in Fig. 4, negligible or small change in cell viability with both low and high concentration of dye is observed

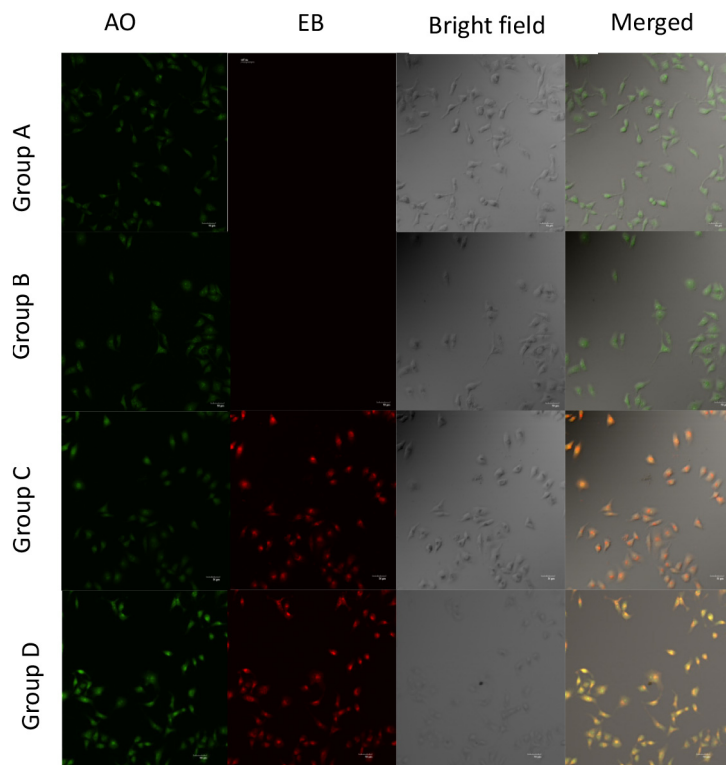


Fig. 5. Confocal imaging after AO/EB staining in PDT process. HepG-2 Cells were incubated with CyO⁻ (20 μM) for 12 h prior to AO/EB staining. Then the HepG-2 cells were irradiated for 20 min under the NIR light Group A: The cells were irradiated for 20 min with no CyO⁻ pre-incubated. Group B: The cells were pre-incubated with CyO⁻ for 12 h but with no irradiation. Group C: The cells were pre-incubated with CyO⁻ for 12 h and irradiated for 20 min and immediately stained with AO/EB. Group D: The cells were pre-incubated with CyO⁻ for 12 h and irradiated for 20 min and continue incubated for 1 h before stained with AO/EB. Scale bar = 20 μm.

without light irradiation, suggesting their low cytotoxicity in the dark. Upon irradiation with an NIR light, the cell viability is gradually decreased with increasing concentrations of CyO^- . Significant cell death is observed for CyO^- at the concentration of 30 μM . In contrast, the CyOH exhibited no similar decrease. The results illustrated that the dye of CyO^- has excellent ability to produce singlet oxygen to kill tumor cells and has great potential in PDT process.

3.5. AO/EB staining

In order to evaluate the feasibility of photosensitizers in visual mode, confocal imaging was performed on confocal microscope in HepG-2 cells. Acridine orange (AO) can penetrate into cells of the cell membrane and embed the nuclear DNA to make it emit bright green fluorescence. Ethidium bromide (EB) can only penetrate the damaged cells of the cell membrane, embed nuclear DNA, and emit orange-red fluorescence. There were four groups of cells that have been treated differently. As shown in Fig. 5, group A was irradiated 20 min with no CyO^- pre-incubated with cells, the cells only showed green fluorescence of AO, while the red fluorescence of EB did not appeared. The result demonstrates that phototoxicity was not caused by irradiation with a 670 nm light source. The cells used in group B were pre-incubated with the CyO^- for 12 h while with no irradiation of near-infrared light. As mentioned above, the cells in this group also showed only green fluorescence, indicating that the CyO^- entering the cells did not induce cell death. At the same concentration and under the same light conditions, the apoptotic cells stained with AO/EB were significantly more stained than the direct staining after 1 h of incubation. All results show that the photosensitizer can be well applied in photodynamic therapy process with low dark toxicity and high phototoxicity.

4. Conclusion

In summary, we have designed and synthesized a unique water soluble Heptamethine cyanine dye for use as a NIR sensitizer for photodynamic therapy. Heptamethine cyanine was selected as the basic fluorescent core due to its NIR emission wavelength and low toxicity. Water-soluble functional group was linked to fluorescent core through multiple methylene flexible chains. 4-amino-2,2,6,6-tetramethylpiperidinyloxy acted as singlet oxygen generating group. Eventually, new NIR photosensitizer was constructed. There were a remarkable absorbance band located 692 nm and emission peaks falls at 762 nm, the quantum yield was calculated for 12.12% in pure aqueous solution using ICG as standards. It has great potential in bio-imaging. The photosensitizer showed excellent properties in PDT process. Singlet oxygen production efficiency of this photosensitizer is 16.98%, which is significantly higher than the previously reported literature. It also shows ultra-low dark toxicity and high phototoxicity in HepG-2 cells. Negligible or small change in cell viability with both low and high concentration of dye is observed without light irradiation. However, significant cell death is observed for CyO^- at the concentration of 30 μM when the dye CyO^- was irradiated with NIR light. The CyO^- also has great ability to penetrate cells with good cell compatibility. In a word, the photosensitizer can be well applied in photodynamic therapy process with low dark toxicity and high phototoxicity.

Declaration of competing interest

There are no conflicts to declare.

Acknowledgements

We thank the financial support from the Fundamental Research Funds for the National Natural Science Foundation of China (No. 61178057).

Appendix A. Supplementary data

Supplementary data to this article can be found online at <https://doi.org/10.1016/j.saa.2019.117702>.

References

- [1] S.M. Usama, S. Thavornpradit, K. Burgess, Optimized heptamethine cyanines for photodynamic therapy, *ACS Appl. Bio Mater.* 1 (2018) 1195–1205.

- [2] M. Bio, P. Rajaputra, Y.J. You, Photodynamic therapy via FRET following bioorthogonal click reaction in cancer cells, *Bioorg. Med. Chem. Lett* 26 (2016) 145–148.
- [3] Q. Cai, J.T. Xu, D. Yang, Y.L. Dai, G.-X. Yang, C.N. Zhong, S.L. Gai, F. He, P.P. Yang, et al., Polypyrrole-coated UCNP@mSiO₂@ZnO nanocomposite for combined photodynamic and photothermal therapy, *J. Mater. Chem. B* 6 (2018) 8148–8162.
- [4] W.J. Xu, J.M. Qian, G.H. Hou, Y.P. Wang, J.L. Wang, T.T. Sun, L.J. Ji, A.L. Suo, Y. Yao, PEGylated hydrazided gold nanorods for pH-triggered chemo/photodynamic/photothermal triple therapy of breast cancer, *Acta Biomater.* 82 (2018) 171–183.
- [5] L. Cao, Q. Wu, Q. Li, S. Shao, Y. Guo, Fluorescence and HPLC detection of hydroxyl radical by a rhodamine-nitroxide probe and its application in cell imaging, *J. Fluoresc.* 24 (2014) 313–318.
- [6] X.W. Huo, Y.M. Jia, D.Y. Liu, L. Gao, L.J. Zhang, L.Y. Li, Y. Qi, L. Cao, Photodynamic diagnosis of gastric cancer using PPHH-CD, *RSC Adv.* 6 (2016) 39216–39224.
- [7] C.L. Sun, J. Li, X.Z. Wang, R. Shen, S. Liu, J.Q. Jiang, T. Li, Q.W. Song, Q. Liao, H.B. Fu, J.N. Yao, H.L. Zhang, Rational design of organic probes for turn-on two-photon excited fluorescence imaging and photodynamic therapy, *Chem* 5 (2019) 600–616.
- [8] H.S. Wang, Development of fluorescent and luminescent probes for reactive oxygen species, *Trac. Trends Anal. Chem.* 85 (2016) 181–202.
- [9] S.S. Wan, J.Y. Zeng, H. Cheng, X.Z. Zhang, ROS-induced NO generation for gas therapy and sensitizing photodynamic therapy of tumor, *Biomaterials* 185 (2018) 51–62.
- [10] J.G. Jo, C.H. Lee, R. Kopelman, X.D., Proc. Lifetime-Resolved Photoacoustic (LPA) Spectroscopy for Monitoring Oxygen Change and Photodynamic Therapy, (PDT), SPIE, 2016 97081L, <https://doi.org/10.1117/12.2213083>.
- [11] X.X. Wang, J.T. Xu, D. Yang, C.Q. Sun, F. He, S.L. Gai, C.N. Zhong, C.X. Li, P.P. Yang, Fe₃O₄@MIL-100(Fe)-UCNPs heterojunction photosensitizer: rational design and application in near infrared light mediated hypoxic tumor therapy, *Chem. Eng. J.* 354 (2018) 1141–1152.
- [12] M. Feng, R.C. Lv, L.Y. Xiao, B. Hu, S.P. Zhu, F. He, P.P. Yang, J. Tian, Highly erbium-doped nanoplatform with enhanced red emission for dual-modal optical-imaging-guided photodynamic therapy, *Inorg. Chem.* 57 (2018) 14594–14602.
- [13] X.L. Zheng, J.C. Ge, J.S. Wu, W.M. Liu, L. Guo, Q.Y. Jia, Y. Ding, H.Y. Zhang, P.F. Wang, Biodegradable hypocrelin derivative nanovesicle as a near-infrared light-driven theranostic for dually photoactive cancer imaging and therapy, *Biomaterials* 185 (2018) 133–141.
- [14] H.P. Tham, K.M. Xu, W.Q. Lim, H.Z. Chen, M.J. Zheng, T.G.S. Thng, S.S. Venkatraman, C.J. Xu, Y.L. Zhao, Microneedle-Assisted topical delivery of photodynamically active mesoporous formulation for combination therapy of deep-seated melanoma, *ACS Nano* 12 (2018) 11936–11948.
- [15] X. Yang, Y. Qian, A NIR facile, cell-compatible fluorescent sensor for glutathione based on Michael addition induced cascade spiroactam opening and its application in hepatocellular carcinoma, *J. Mater. Chem. B* 6 (2018) 7486–7494.
- [16] B. Zhou, Y. Li, G. Niu, M. Lan, Q. Jia, Q. Liang, Near-infrared organic dye-based nanoagent for the photothermal therapy of cancer, *ACS Appl. Mater. Interfaces* 8 (2016) 29899–29905.
- [17] Q. Yang, C. Jia, Q. Chen, W. Du, Y. Wang, Q. Zhang, A NIR fluorescent probe for the detection of fluoride ions and its application in in vivo bioimaging, *J. Mater. Chem. B* 5 (2017) 2002–2009.
- [18] A.T. Wrobel, T.C. Johnstone, A. Deliz Liang, S.J. Lippard, P. Rivera-Fuentes, J. Am. Chem. Soc. 136 (2014) 4697–4705.
- [19] L. Liu, Z. Ruan, T.W. Li, P. Yuan, L.F. Yan, Near infrared imaging-guided photodynamic therapy under an extremely low energy of light by galactose targeted amphiphilic polypeptide micelle encapsulating BODIPY-Br-2, *Biomater. Sci.* 4 (2016) 1638–1645.
- [20] T.T. Jing, L.Y. Fu, L. Liu, L.F. Yan, A reduction-responsive polypeptide nanogel encapsulating NIR photosensitizer for imaging-guided photodynamic therapy, *Polym. Chem.* 7 (2016) 951–957.
- [21] X. Hu, H.L. Tian, W. Jiang, A.X. Song, Z.H. Li, Y.X. Luan, Rational design of IR820- and Ce6-based versatile micelle for single NIR laser-induced imaging and dual-modal phototherapy, *Small* 14 (1–10) (2018) 1802994.
- [22] C.M. Huang, Y. Qian, CT-BODIPY with donor-acceptor architecture: red-AIE property and selective interaction with BSA, *ChemistrySelect* 4 (2019) 2205–2210.
- [23] L.F. Wang, Y. Qian, A novel quinoline-BODIPY fluorescent probe for fast sensing biothiols via hydrogen bonds assisted-deprotonation mechanism and its application in cells and zebrafish imaging, *J. Photochem. Photobiol. A Chem.* 372 (2019) 122–130.
- [24] J. Lee, Y.H. Lee, C.B. Jeong, J.S. Choi, K.S. Chang, M. Yoon, Gold nanorods-conjugated TiO₂ nanoclusters for the synergistic combination of phototherapeutic treatments of cancer cells, *J. Nanobiotechnol.* 16 (2018) 104.
- [25] Y. Zhang, T. Lv, H. Zhang, X. Xie, Z. Li, H. Chen, Y. Gao, Folate and heptamethine cyanine modified chitosan-based nanotheranostics for tumor targeted near-infrared fluorescence imaging and photodynamic therapy, *Biomacromolecules* 18 (2017) 2146–2160.
- [26] J. Mikkila, E. Anaya-Plaza, V. Liljestrom, J.R. Caston, T. Torres, A. de la Escosura, M.A. Kostianen, Hierarchical organization of organic dyes and protein cages into photoactive crystals, *ACS Nano* 10 (2016) 1565–1571.
- [27] X. Qu, F. Yuan, Z. He, Y. Mai, J. Gao, X. Li, D. Yang, Y. Cao, X. Li, Z. Yuan, A rhodamine-based single-molecular theranostic agent for multiple-functionality tumor therapy, *Dyes Pigments* 166 (2019) 72–83.
- [28] C. Shi, J.B. Wu, D. Pan, Review on near-infrared heptamethine cyanine dyes as theranostic agents for tumor imaging, targeting, and photodynamic therapy, *J. Biomed. Opt.* 21 (2016) 50901.
- [29] L.Q. Gao, C.R. Zhang, D. Gao, H. Liu, X.H. Yu, J.H. Lai, F. Wang, J. Lin, Z.F. Liu, Enhanced anti-tumor efficacy through a combination of integrin alpha v beta 6-targeted photodynamic therapy and immune checkpoint inhibition, *Theranostics* 6 (2016) 627–637.
- [30] C.J. Wang, Y. Qian, A novel BODIPY-based photosensitizer with pH-active singlet oxygen generation for photodynamic therapy in lysosomes, 17 (2019) 8001–8007.

- [31] L.F. Wang, J. Bai, Y. Qian, A triphenylamine-BODIPY photosensitizer with D-A configuration and its intracellular simulated photodynamic therapy application, *New J. Chem.* (2019) <https://doi.org/10.1039/c9nj04166d>.
- [32] N. Molupe, B. Babu, D.O. Oluwole, E. Prinsloo, J. Mack, T. Nyokong, The investigation of in vitro dark cytotoxicity and photodynamic therapy effect of a 2,6-dibromo-3,5-distyryl BODIPY dye encapsulated in Pluronic® F-127 micelles, *J. Coord. Chem.* 71 (2018) 3444–3457.
- [33] M.H. Sakr, N.M. Halabi, L.N. Kalash, S.I. Al Ghadban, M.K. Rammah, M.E. El Sabban, K.H. Bouhadir, T.H. Ghaddar, Synthesis and in vitro cytotoxicity evaluation of ruthenium polypyridyl-sensitized paramagnetic titania nanoparticles for photodynamic therapy, *RSC Adv.* 6 (2016) 47520–47529.
- [34] L. Jiao, F. Song, J. Cui, X. Peng, A near-infrared heptamethine aminocyanine dye with a long-lived excited triplet state for photodynamic therapy, *Chem. Commun.* 54 (2018) 9198–9201.
- [35] F. Yu, P. Song, P. Li, B. Wang, K. Han, Development of reversible fluorescence probes based on redox oxoammonium cation for hypobromous acid detection in living cells, *Chem. Commun.* 48 (2012) 7735–7737.
- [36] David O. Oluwole, Earl Prinsloo, Tebello Nyokong, Photophysical properties of nanoconjugates of zinc(II) 2(3)-mono-2-(4-oxy)phenoxy)acetic acid phthalocyanine with cysteamine capped silver and silver-gold nanoparticles, *Polyhedron* 119 (2016) 434–444.
- [37] X. Yang, Y. Qian, A near-infrared fluorescent probe for the discrimination of cysteine in pure aqueous solution and imaging of cysteine in hepatocellular carcinoma cells with facile cell-compatible ability, *New J. Chem.* 43 (2019) 3725–3732.
- [38] L.L. Tong, Y. Qian, A naphthalimide-rhodamine chemodosimeter for hypochlorite based on TBET: high quantum yield and endogenous imaging in living cells, *J. Photochem. Photobiol. A Chem.* 368 (2019) 62–69.